Hydrothermal Deposition of ZnO Nanoparticles on 3D-Printed Polymer Scaffolds for Enhanced Photocatalysis

*Ahmet Yavaş**
İzmir Kâtip Çelebi University, Department of Metallurgical and Materials Engineering, İzmir, Türkiye
**Corresponding author: ahmet.yavas@ikcu.edu.tr*

Abstract

In this study, ZnO nanowires were successfully synthesized on 3D-printed epoxy-based polymer scaffolds via a hydrothermal method. A ZnO seed layer was first deposited onto the 3D-printed structures fabricated by digital light processing (DLP), followed by hydrothermal growth to form nanowires. Structural and surface analyses were carried out using X-ray Diffraction (XRD), Scanning Electron Microscopy (SEM), and X-ray photoelectron spectroscopy (XPS). SEM revealed that flower-like ZnO nanowire clusters with rod-like morphology were uniformly distributed over the scaffold surface. XRD confirmed the formation of wurtzite-phase crystalline ZnO, and XPS verified the presence of Zn^{2+} and O^{2-} chemical states consistent with ZnO formation. The photocatalytic performance of the scaffolds was evaluated through the degradation of methylene blue (MB) under artificial sunlight. The ZnO-coated samples exhibited significantly improved photocatalytic activity, achieving an apparent rate constant of about 0.28 h^{-1} and a maximum degradation efficiency of 81.36% after 6 hours, outperforming both the neat scaffold and the catalyst-free control. These results demonstrate the potential of ZnO-integrated 3D-printed scaffolds for practical photocatalytic applications.

Keywords: Photocatalysis, 3D printing, digital light processing, hydrothermal synthesis, zinc oxide

Introduction

In recent decades, environmental concerns have gained increasing prominence due to rapid industrialization, sustained economic growth, technological advancements, and population expansion. One of the most critical challenges is the contamination of water resources by organic pollutants, which necessitates the development of efficient and sustainable treatment technologies (Pivert et al., 2022; Yavaş et al., 2024).

Among various methods employed for wastewater treatment—such as adsorption, biodegradation, and ozonolysis—photocatalysis has emerged as a particularly promising technique due to its environmental compatibility, high degradation efficiency, and relatively low cost. Zinc oxide (ZnO) is widely recognized as a potent photocatalyst because of its strong oxidative potential, chemical stability, and non-toxicity (Rasheed et al., 2025). With its wide bandgap, ZnO can generate electron-hole pairs under UV irradiation, enabling the breakdown of a wide range of organic pollutants (Sanakousar et al., 2022). However, the practical use of ZnO in powdered form often requires additional separation steps after treatment, increasing process complexity and the risk of secondary contamination (Canon, 2015).

To overcome these limitations, recent studies have focused on immobilizing ZnO onto 3D-printed supports to improve catalyst reusability and operational convenience. For instance, Son et al. fabricated ZnO-based hierarchical structures on FDM-printed backbones for efficient methylene blue degradation (Son et al., 2018). Sevastaki et al. used PLA scaffolds with eco-friendly ZnO coatings to remove paracetamol from water (Sevastaki et al., 2021). Vrithias et al. demonstrated the photocatalytic effectiveness of Mn-doped ZnO on HDPE sponges against detergent pollutants (Vrithias et al., 2023). Verma et al. grew ZnO nanowires on pyrolyzed carbon microlattices fabricated via DLP printing, achieving high efficiency and recyclability (Verma et al., 2025). Kumbhakar et al. printed PLA-based porous architectures and coated them with ZnO nanosheets, showing fast dye degradation through a synergistic mechanism of adsorption and photodegradation, while also demonstrating stable reuse without ZnO leaching (Kumbhakar et al., 2021).

In contrast to these approaches, the present study introduces a distinct methodology by utilizing DLP-based vat photopolymerization to fabricate high-resolution, porous scaffolds from an epoxy/acrylate-based photo-curable resin (Ngo et al., 2018). This material system offers several advantages over conventional PLA or HDPE matrices, including enhanced UV-curability, mechanical strength, and chemical stability—making it ideal for photocatalytic applications (Baronins et al., 2023).

Furthermore, ZnO nanoparticles are grown in situ via hydrothermal synthesis after the printing process, ensuring a uniform and stable coating without compromising the structural complexity of the scaffold (Phasa et al., 2024).

To the best of our knowledge, this is the first study combining DLP-printed epoxy/acrylate scaffolds with post-synthetic hydrothermal ZnO growth for photocatalytic applications. The resulting structures offer improved surface area exposure, ease of handling, and reusability. Characterization was performed using XRD, SEM, and XPS techniques, and photocatalytic performance was assessed through the degradation of methylene blue under UV light. These findings underline the potential of this novel fabrication route for developing scalable, reusable, and efficient water treatment systems.

Materials and Methods

Materials

In this study, a clear UV-sensitive resin manufactured by Hongkong Anycubic Technology Co., Limited was employed as the liquid resin. Based on the manufacturer's data sheets, the epoxy/acrylate-based formulation of the resin comprises phenolic epoxy resin (60%), tri(propylene glycol) diacrylate (35%), and 1-hydroxycyclohexyl phenyl ketone (5%), with corresponding CAS numbers 61788-97-4, 42978-66-5, and 947-19-3, respectively. Zinc acetate dihydrate ($Zn(CH_3COO)_2 \cdot 2H_2O$) and sodium hydroxide (NaOH) were used as precursors in the dip-coating process, while zinc nitrate hexahydrate ($Zn(NO_3)_2 \cdot 6H_2O$) and hexamethylenetetramine ($C_6H_{12}N_4$) were employed for the hydrothermal synthesis. Methylene blue (MB) was utilized as the model dye for photocatalytic activity tests. All chemicals were purchased from Sigma-Aldrich and used without further purification. Distilled water was used throughout all experimental procedures.

Method

SolidWorks software was employed to design 3D computer-aided design (CAD) models of the scaffolds, which were then exported in STL format. The slicing and G-code generation for the models were carried out using HALOT BOX, a slicer software specific for resin-based 3D printing. The composite scaffolds were fabricated using a commercial LCD-based stereolithography (SLA) printer (Creality Halot-One). The printing parameters were fixed for all samples, with a layer thickness of 50 μm and an exposure time of 4 seconds per layer. After the printing process, the samples were immersed in isopropyl alcohol (IPA) and washed for 10 minutes to eliminate residual uncured resin. Post-curing was performed for 60 minutes to ensure complete polymerization and mechanical stability of the scaffolds.

To prepare the ZnO seeding layer, 25 mg of zinc acetate dihydrate and 10 mg of sodium hydroxide were each dissolved in 100 mL of ethanol. The resulting solution was stirred at room temperature for 1.5 hours. The 3D-printed scaffolds were then vertically immersed in the seeding solution for 10 minutes to enable surface deposition of ZnO precursors. After deposition, the scaffolds were heated at 50 °C for 10 minutes to fix the seed layer. This seeding process was repeated three times to ensure uniform coverage.

Subsequently, the hydrothermal growth of ZnO nanowires was carried out by immersing the seeded scaffolds into an equimolar aqueous solution (30 mM) of zinc nitrate hexahydrate and hexamethylenetetramine, contained in a Teflon-lined stainless steel autoclave. The reaction was conducted at 90 °C for 4 hours to promote the controlled growth of ZnO nanostructures. Following synthesis, the scaffolds were rinsed thoroughly with distilled water and dried at 60 °C. A final heat treatment at 110 °C for 180 minutes was applied to enhance the crystallinity of the ZnO nanowires. The preparation stages of ZnO-coated 3D-printed polymer scaffolds were schematically represented in Figure 1.

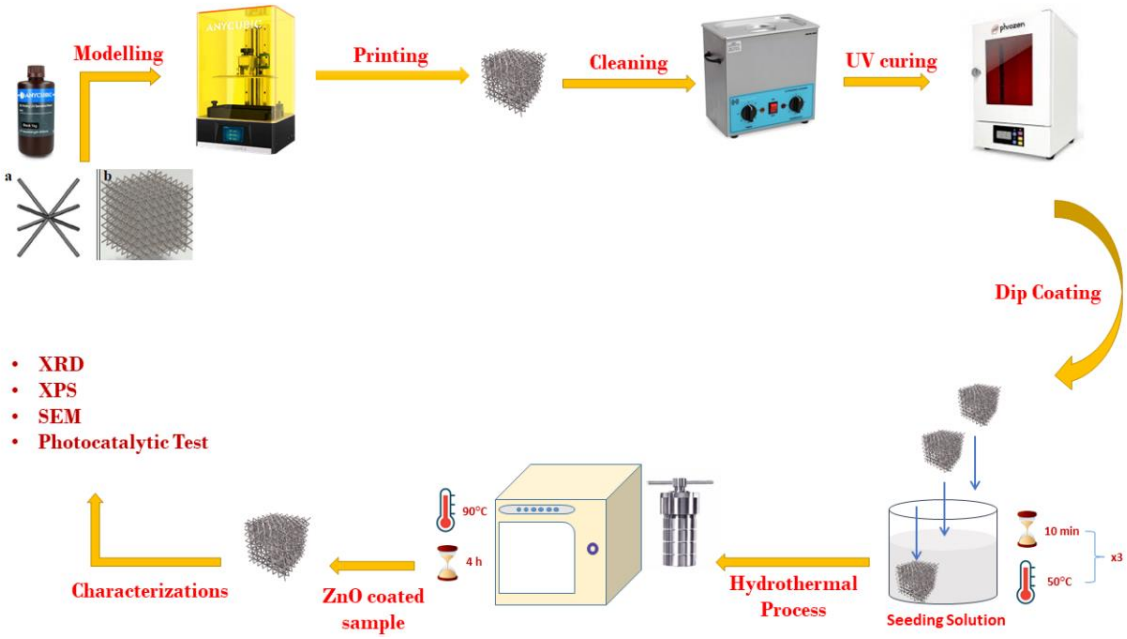

Figure 1. Schematic representation of the preparation stages of ZnO-coated 3D-printed polymer scaffolds

Characterization

The structural analysis of both uncoated – neat (epoxy) sample - and ZnO-coated 3D-printed polymer scaffolds was performed using XRD with a Bruker AXS D2 Phaser diffractometer, operating with monochromatic Cu-Kα radiation (λ = 1.54178 Å). The crystallographic phases and the presence of ZnO were identified by comparing the diffraction patterns. The surface morphology of the scaffold surfaces were examined using SEM with a Carl Zeiss EVO 300VP instrument. In addition, XPS analysis was conducted using a Thermo Scientific K-Alpha system to investigate the surface chemical composition and bonding states of the neat and ZnO coated scaffolds.

Photocatalytic Experiments

The photocatalytic performance of the uncoated and ZnO-coated 3D-printed scaffolds was evaluated by monitoring the degradation of MB, a model organic pollutant, under artificial sunlight. An initial MB solution with a concentration of 2.5 ppm (7.5×10^{-6} M) was prepared, and 30 mL of this solution was used for each test. To assess the adsorption effect, the scaffolds were first immersed in the MB solution and kept in the dark for 30 mins. The concentration of MB was monitored using a UV–Vis spectrophotometer (Shimadzu UV-1240) at 664 nm. Following the adsorption–desorption equilibrium, samples were exposed to artificial sunlight (Osram UltraVitalux E27, 300 W) placed 25 cm above the beakers for 6 hours without stirring. Control experiments without any catalyst were also conducted for comparison. Absorbance values were recorded at regular intervals to evaluate the photocatalytic degradation efficiency.

Results and Discussion

Phase analysis

The XRD patterns of the neat (uncoated) and ZnO-coated 3D-printed epoxy scaffolds are presented in Figure 2. The neat polymer scaffold exhibits a broad diffraction hump centered around 18°–25°, which is characteristic of the amorphous nature of the photo-curable epoxy resin used in the 3D printing process (Rudresh et al., 2019). In contrast, the ZnO-coated sample shows distinct and sharp diffraction peaks located at approximately 32.3°, 35.0°, and 36.9°, corresponding to the (100), (002), and (101) planes of hexagonal wurtzite ZnO (JCPDS No. 36-1451), respectively. The appearance of these peaks confirms the successful formation and crystalline nature of the ZnO phase on the scaffold surface. The intensity and sharpness of these peaks indicate a high degree of crystallinity and preferred orientation of ZnO nanostructures grown via hydrothermal synthesis. These findings validate the structural integrity of ZnO on the 3D-printed scaffold and suggest that the hydrothermal process effectively deposited crystalline ZnO without altering the bulk amorphous structure of the epoxy matrix.

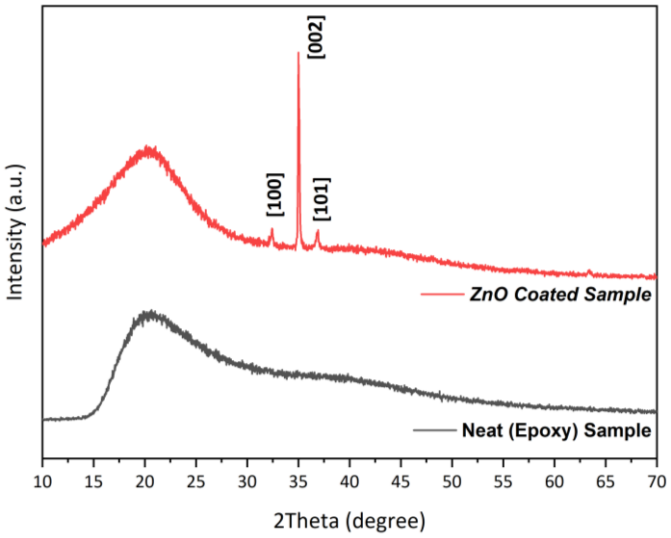

Figure 2. Phase structures of the uncoated and ZnO-coated 3D-printed epoxy scaffolds

Surface chemistry of ZnO coated sample

The surface chemical composition and elemental states of the ZnO-coated 3D-printed scaffolds were analyzed by X-ray photoelectron spectroscopy. The wide-scan survey spectrum (Figure 3a) confirms the presence of key elements, including Zn, O, C, and N, as well as minor traces of Na and Cl, which may originate from precursor residues or environmental contamination. The distinct Zn2p and O1s peaks are indicative of ZnO formation on the scaffold surface, while the C1s and N1s signals are attributed to the polymer matrix and possible surface adsorbates.

A high-resolution scan of the Zn2p region (Figure 3b) further verifies the presence of Zn in the ZnO phase. The spectrum displays two prominent peaks located at binding energies of 1021.38 eV and 1044.47 eV, corresponding to Zn 2p$_{3/2}$ and Zn 2p$_{1/2}$, respectively. The observed spin–orbit splitting of 23.09 eV is consistent with the typical values reported for Zn^{2+} in ZnO, confirming the successful formation of ZnO with the expected oxidation state (Akalın et al., 2024; Sakar et al., 2025). These XPS findings provide strong evidence for the effective hydrothermal growth of ZnO nanostructures on the surface of the polymeric scaffold, further supporting the results obtained from XRD analysis.

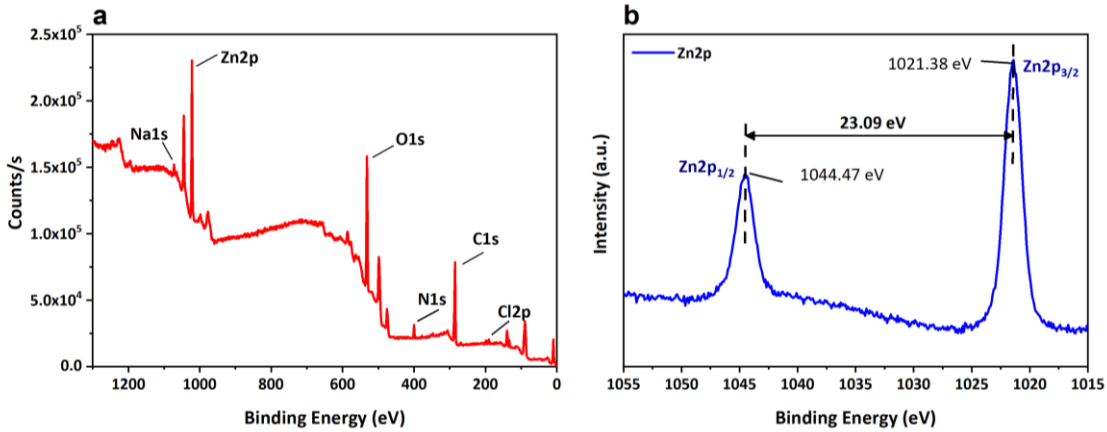

Figure 3. **(a)** XPS survey spectrum and **(b)** high-resolution peaks of Zn for the ZnO-coated 3D-printed sample

Surface morphology of ZnO coated sample

The surface morphology of the 3D-printed ZnO-coated scaffolds was examined using scanning electron microscopy (SEM), and the results are presented in Figure 4.

Figure 4a shows the low-magnification (8.5X) image of the entire 3D-printed scaffold, revealing its well-defined, interconnected lattice architecture. The printed polymer framework exhibits a uniform geometry, indicating successful fabrication via the DLP technique. In Figure 4b, a 200X magnification

image reveals the surface of the scaffold struts, where early-stage nucleation and regionally distributed ZnO nanostructures can be observed. These nanowire clusters appear as dense deposits on the outer layers of the polymer filaments, suggesting a localized and surface-driven growth behavior during hydrothermal synthesis. Irmak et al. reported a similar nanowire morphology, where ZnO nanowires were hydrothermally synthesized on carbon fibers. Their SEM analysis demonstrated vertically aligned, dense nanowire structures with comparable thickness and length ranges, supporting the consistency and effectiveness of hydrothermal synthesis for producing ZnO nanowires on various substrates (Tunç et al., 2020). A higher magnification image at 1000X (Figure 4c) provides a closer view of the ZnO nanowire morphology. The nanostructures are seen forming flower-like clusters, covering portions of the scaffold surface, which likely enhance surface area and reactivity for photocatalytic applications. Finally, Figure 4d presents a high-resolution SEM image at 25000X magnification, showing individual ZnO nanowires in detail. The nanowires exhibit uniform, rod-like morphology with diameters ranging approximately from 108 nm to 257 nm, as measured from selected regions. This confirms the successful growth of well-aligned ZnO nanowires with nanoscale dimensions and good coverage on the polymeric substrate. These SEM observations, in combination with XRD and XPS results, confirm the effective integration of ZnO nanostructures onto the 3D-printed scaffolds and the potential of the resulting composite for enhanced photocatalytic activity.

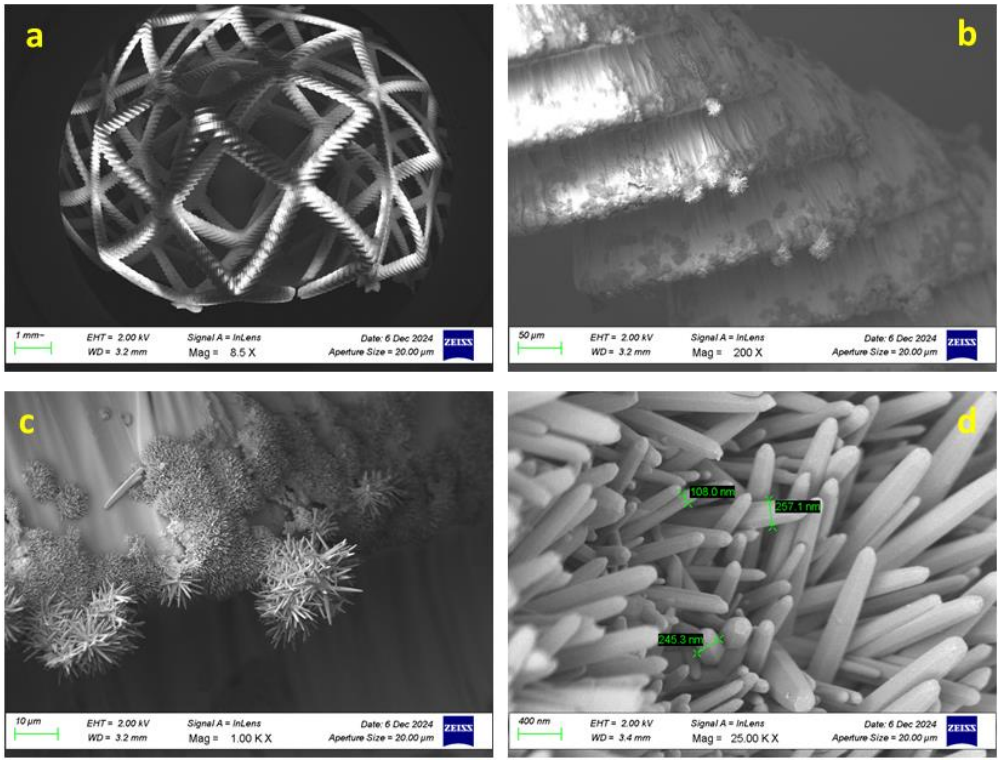

Figure 4. SEM images of the ZnO-coated 3D-printed sample in different magnifications; **(a)** 8.5X, **(b)** 200X, **(c)** 1000X, and **(d)** 25000X

Photocatalytic performance

The photocatalytic activity of the neat and ZnO-coated 3D-printed scaffolds was evaluated by monitoring the degradation of methylene blue solution under artificial sunlight irradiation.

As shown in Figure 5a, the apparent kinetic rate constants (k_{app}), derived from pseudo-first-order kinetics based on the Langmuir–Hinshelwood (L–H) model (Kumar et al., 2008), demonstrate a significant enhancement in photocatalytic activity with the introduction of ZnO nanostructures. The correlation of all kinetic curves to the pseudo-first-order model exceeded $R^2 > 0.97$, validating the reliability of the applied kinetic analysis (Yavaş et al., 2022). The ZnO-coated sample exhibited the highest rate constant (~2.8×10^{-1} h^{-1}), which is more than twice that of the uncoated scaffold (~1.3×10^{-1} h^{-1}) and over three times higher than the reference solution (~0.9×10^{-1} h^{-1}) without any catalyst.

The performance of the reference (Ref) solution, which achieved a kinetic response despite the absence of any solid catalyst, is attributed to direct photolysis of MB molecules under UV-rich artificial sunlight (Appia et al., 2025). The neat (uncoated) scaffold, on the other hand, showed a modest increase in the reaction rate, which may stem from a combination of limited dye adsorption onto the polymer

surface and potential light scattering effects induced by the porous 3D structure of the scaffold. These physical contributions likely enhanced the local interaction between incident light and MB molecules, slightly promoting degradation beyond that of pure photolysis.

The corresponding photocatalytic removal efficiencies after 6 hours of illumination are presented in Figure 5b. The ZnO-coated scaffold achieved an MB degradation efficiency of 81.36%, compared to 42.2% for the neat polymer scaffold and only 33.45% for the reference. This notable enhancement is attributed to the presence of hydrothermally grown, crystalline ZnO nanowires with high surface area and photoactivity (Zhang et al., 2016). Bourfaa et al. investigated hydrothermally grown ZnO nanorods on glass substrates and reported photodegradation rate constants exceeding 0.2 h^{-1} for MB under UV irradiation, demonstrating performance highly comparable to our ZnO-coated 3D-printed scaffolds (Bourfaa et al., 2018).

The increased surface roughness and effective dispersion of ZnO, as evidenced by SEM and XPS analyses, likely contributed to the improved interaction between the catalyst surface and organic dye molecules. These results confirm that immobilizing ZnO on 3D-printed porous scaffolds not only eliminates the need for post-treatment separation of powder catalysts but also enhances light absorption and surface interaction, making the composite structure a promising candidate for practical photocatalytic water treatment applications.

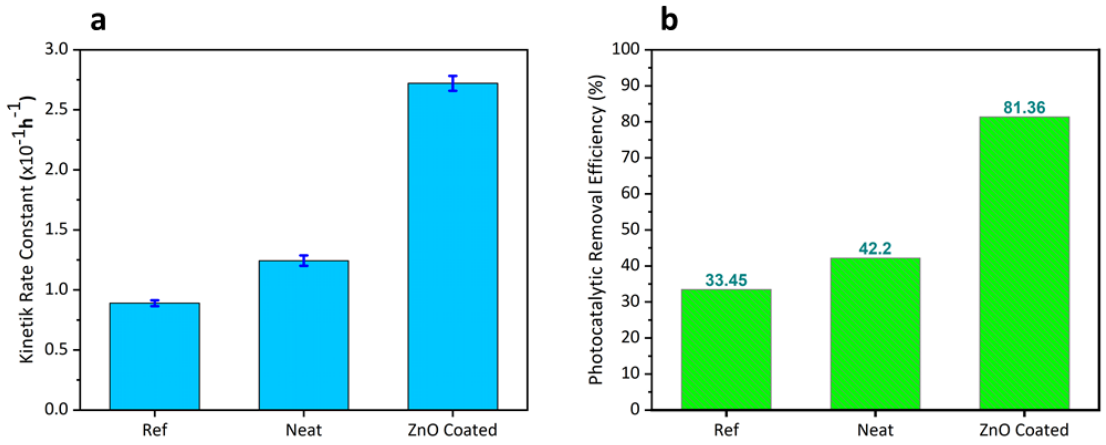

Figure 5. Photocatalytic degradation rates **(a)** and MB removal performances **(b)** of samples

Conclusions

This work presents a novel approach to fabricating photocatalytically active 3D-printed scaffolds by integrating hydrothermally synthesized ZnO nanowires onto DLP-printed epoxy-based substrates. Morphological analysis showed dense and uniform ZnO nanowire formation, while XRD and XPS confirmed the formation of crystalline ZnO with the expected chemical states. Photocatalytic degradation experiments using methylene blue demonstrated that the ZnO-coated scaffolds significantly enhanced dye degradation compared to uncoated and control samples. The optimized sample achieved a rate constant of approximately 0.28 h^{-1} and a degradation efficiency of 81.36% under 6 hours of UV-rich artificial sunlight. This enhancement is attributed to the increased surface area, better light absorption, and strong interaction between the nanostructured ZnO and the dye molecules. Overall, the findings suggest that such composite architectures are promising candidates for scalable and reusable photocatalytic systems in wastewater treatment applications.

References

[1] Akalın, S. A., Yavaş, A., Güler, S., & Erol, M. (2024). Photocatalytic activities of Fe2O3 coated ZnO nanowires grown by electrochemical anodization method. Ceramics International, 50(20), 39278–39284. https://doi.org/10.1016/J.CERAMINT.2024.07.298

[2] Appia, F. T. A., Kouassi, T. G. D., Kimou, K. J., Coulibaly, C. S., Meledje, J.-C., & Ouattara, L. (2025). Photolytic Degradation of Methylene Blue: The Effect of Various Factors on Wastewater Treatment Efficiency. Asian Journal of Chemical Sciences, 15(1), 41–52. https://doi.org/10.9734/AJOCS/2025/V15I1347

[3] Baronins, J., Antonov, M., Abramovskis, V., Rautmane, A., Lapkovskis, V., Bockovs, I., Goel, S., Thakur, V. K., & Shishkin, A. (2023). The Effect of Zinc Oxide on DLP Hybrid Composite

Manufacturability and Mechanical-Chemical Resistance. Polymers 2023, Vol. 15, Page 4679, 15(24), 4679. https://doi.org/10.3390/POLYM15244679

[4] Bourfaa, F., Boutelala, A., Salah, A. M., Attaf, N., & Ocak, Y. S. (2018). Effect of deposition tıme of zno nanorods by hydrothermal method on photocatalysis activity. International Journal of Health Services Research and Policy, 3(1), 33–39. https://doi.org/10.23884/IJHSRP.2018.3.1.04

[5] Canon, A. (2015). Nanostructured ZnO films for water treatment by photocatalysis.

[6] Kumar, K. V., Porkodi, K., & Rocha, F. (2008). Langmuir–Hinshelwood kinetics – A theoretical study. Catalysis Communications, 9(1), 82–84. https://doi.org/10.1016/J.CATCOM.2007.05.019

[7] Kumbhakar, P., Ambekar, R. S., Mahapatra, P. L., & Sekhar Tiwary, C. (2021). Quantifying instant water cleaning efficiency using zinc oxide decorated complex 3D printed porous architectures. Journal of Hazardous Materials, 418, 126383. https://doi.org/10.1016/J.JHAZMAT.2021.126383

[8] Ngo, T. D., Kashani, A., Imbalzano, G., Nguyen, K. T. Q., & Hui, D. (2018). Additive manufacturing (3D printing): A review of materials, methods, applications and challenges. Composites Part B: Engineering, 143, 172–196. https://doi.org/10.1016/J.COMPOSITESB.2018.02.012

[9] Phasa, A., Aini, Q., Yasin Siregar, M., Sabilla, S., Triyadi, D., Aflaha, R., Ghulam, M., Khan, I., & Nurfani, E. (2024). Photocatalytic degradations of organic pollutants in wastewater using hydrothermally grown ZnO nanoparticles. Greensusmater, 1(2), 39–43. https://doi.org/10.62755/GREENSUSMATER.2024.1.2.39-43

[10] Pivert, M. Le, Martin, N., & Leprince-Wang, Y. (2022). Hydrothermally Grown ZnO Nanostructures for Water Purification via Photocatalysis. Crystals 2022, Vol. 12, Page 308, 12(3), 308. https://doi.org/10.3390/CRYST12030308

[11] Rasheed, H. M., Aroosh, K., Meng, D., Ruan, X., Akhter, M., & Cui, X. (2025). A review on modified ZnO to address environmental challenges through photocatalysis: Photodegradation of organic pollutants. Materials Today Energy, 48, 101774. https://doi.org/10.1016/J.MTENER.2024.101774

[12] Rudresh, M., Maruthi, B. H., Channakeshavalu, K., & Nagaswarupa, H. P. (2019). Mechanical and thermal behavior of epoxy based halloysite nano clay/PMMA hybrid nanocomposites. SN Applied Sciences, 1(7), 1–8. https://doi.org/10.1007/S42452-019-0749-0/FIGURES/12

[13] Sakar, N., Akalin, S. A., Yavas, A., Zeyrek, M., Kose, P., & Oguzlar, S. (2025). Ce and Gd doped ZnO nanorods: A study on structural, optical, and photocatalytic enhancements. Journal of Alloys and Compounds, 1021, 179672. https://doi.org/10.1016/J.JALLCOM.2025.179672

[14] Sanakousar, F. M., Vidyasagar, C., Jiménez-Pérez, V. M., & Prakash, K. (2022). Recent progress on visible-light-driven metal and non-metal doped ZnO nanostructures for photocatalytic degradation of organic pollutants. Materials Science in Semiconductor Processing, 140, 106390. https://doi.org/10.1016/J.MSSP.2021.106390

[15] Sevastaki, M., Papadakis, V. M., Romanitan, C., Suchea, M. P., & Kenanakis, G. (2021). Photocatalytic Properties of Eco-Friendly ZnO Nanostructures on 3D-Printed Polylactic Acid Scaffolds. Nanomaterials 2021, Vol. 11, Page 168, 11(1), 168. https://doi.org/10.3390/NANO11010168

[16] Son, S., Jung, P. H., Park, J., Chae, D., Huh, D., Byun, M., Ju, S., & Lee, H. (2018). Customizable 3D-printed architecture with ZnO-based hierarchical structures for enhanced photocatalytic performance. Nanoscale, 10(46), 21696–21702. https://doi.org/10.1039/C8NR06788K

[17] Tunç, I. D., Erol, M., Güneş, F., & Sütçü, M. (2020). Growth of ZnO nanowires on carbon fibers for photocatalytic degradation of methylene blue aqueous solutions: An investigation on the optimization of processing parameters through response surface methodology/central composite

design. Ceramics International, 46(6), 7459–7474. https://doi.org/10.1016/J.CERAMINT.2019.11.244

[18] Verma, G., Islam, M., & Gupta, A. (2025). ZnO nanowire-decorated 3D printed pyrolytic carbon for solar light–driven photocatalytic degradation of wastewater contaminants. Advanced Composites and Hybrid Materials, 8(1), 1–17. https://doi.org/10.1007/S42114-024-01125-9/METRICS

[19] Vrithias, N. R., Katsara, K., Papoutsakis, L., Papadakis, V. M., Viskadourakis, Z., Remediakis, I. N., & Kenanakis, G. (2023). Three-Dimensional-Printed Photocatalytic Sponges Decorated with Mn-Doped ZnO Nanoparticles. Materials, 16(16), 5672. https://doi.org/10.3390/MA16165672/S1

[20] Yavaş, A., Güneş, F., Erol, M., Sütçü, M., Güler, S., Torman Kayalar, M., & Keskin, Ö. Y. (2022). Development of visible light active self-cleaning clay roofing tiles as novel building materials: An investigation on the effects of α-Fe2O3 coating and firing temperature. Journal of Cleaner Production, 362, 132302. https://doi.org/10.1016/J.JCLEPRO.2022.132302

[21] Yavaş, A., Güneş, F., Erol, M., Sütçü, M., & Özdemir, E. T. (2024). Visible light-induced self-cleaning ZnO coated-clay roofing tiles: The role of coating concentration on structural and photocatalytic properties. Surfaces and Interfaces, 46, 103975. https://doi.org/10.1016/J.SURFIN.2024.103975

[22] Zhang, F., Chen, X., Wu, F., & Ji, Y. (2016). High adsorption capability and selectivity of ZnO nanoparticles for dye removal. Colloids and Surfaces A: Physicochemical and Engineering Aspects, 509, 474–483. https://doi.org/10.1016/J.COLSURFA.2016.09.059